

Experimental relation between particle and energy confinement in reversed-field pinches

Sara Mazur and Peter Nordlund

Department of Fusion Plasma Physics, The Alfvén Laboratory, Royal Institute of Technology, S-100 44 Stockholm, Sweden

Klaus-Dieter Zastrow

Department of Physics I, Royal Institute of Technology, S-100 44 Stockholm, Sweden

Jerzy H. Brzozowski and James R. Drake

Department of Fusion Plasma Physics, The Alfvén Laboratory, Royal Institute of Technology, S-100 44 Stockholm, Sweden

(Received 16 March 1993)

Confinement studies have been performed on the high-aspect-ratio, high-current-density Extrap-T1 (Stockholm) reversed-field pinch. Experimental evidence is presented that the scaling of the particle confinement time is not dominated by the dynamo activity. This results in an anticorrelation between particle confinement time and energy confinement time, which becomes apparent in this experiment, as the ratio of Spitzer to total input power is varied over the wide range 0.4–0.8.

PACS number(s): 52.55.Hc, 52.55.Pi, 52.25.Fi

The reversed-field pinch (RFP) [1, 2] is a toroidal axisymmetric confinement scheme with several attractive advantages such as weak magnetic field at external windings, high β , compact size, and the possibility for Ohmic heating to ignition. In contrast to the tokamak, the toroidal field is generated almost entirely by internal currents. The field configuration of an RFP is sustained against dissipative losses by a mechanism, known as the dynamo, which couples the externally applied toroidal electric field to the poloidal current. It has been shown that such coupling can be provided by current-driven magnetohydrodynamic (MHD) instabilities (resistive tearing modes [3–5]) and by energetic electron flow along stochastic field lines [6]. In this context, a non-Spitzer component of the loop voltage is required for the dynamo to sustain the RFP configuration. It is anticipated that the MHD relaxation process and the associated stochastization of the magnetic field lines of force should strongly affect the particle confinement properties of reversed-field pinches.

In this Rapid Communication, we present experimental evidence that the scaling of the particle confinement time τ_p is not dominated by the dynamo activity. The experiments have been performed on the high-aspect-ratio Extrap-T1 RFP ($R_0/a = 0.5 \text{ m}/0.057 \text{ m} = 8.8$, where R_0 is the major radius, and a is the minor radius of the torus) [7]. The maximum average toroidal current density is 10 MA/m^2 , a factor of 2 higher than in other RFP experiments. The effects of Spitzer input power P_S and non-Spitzer input power $P - P_S$ on particle confinement time τ_p and energy confinement time τ_E are studied over the wide range of P_S/P from 0.4 to 0.8. We relate the Spitzer resistivity η_S to the Spitzer resistance R_S using the polynomial function model [8] to account for the helical current path. The Spitzer resistivity is calculated from the spectroscopically measured effective ionic charge Z_{eff} . In the figures presented here, each symbol represents an ensemble average value of data from 20 consecutive discharges taken during the flat-top phase, and the error bars represent three times the standard deviation of the ensemble averages.

A typical discharge is shown in Fig. 1.

In one series of experiments, the toroidal plasma current I_ϕ was varied in the range 40–100 kA, with pinch parameter $\Theta = B_\theta(a)/\langle B_\phi \rangle \approx 1.7$. Here, $B_\theta(a)$ is the poloidal magnetic field at the edge, and $\langle B_\phi \rangle$ is the cross-sectionally averaged toroidal magnetic field. Within this current scan, the current to line density ratio I/N was varied in the range 0.7×10^{-13} – $1.6 \times 10^{-13} \text{ A m}$. In Fig. 2 we show line average electron temperature T_e from line intensity ratios of Li-like oxygen and line average electron density n_e measured by interferometry, together

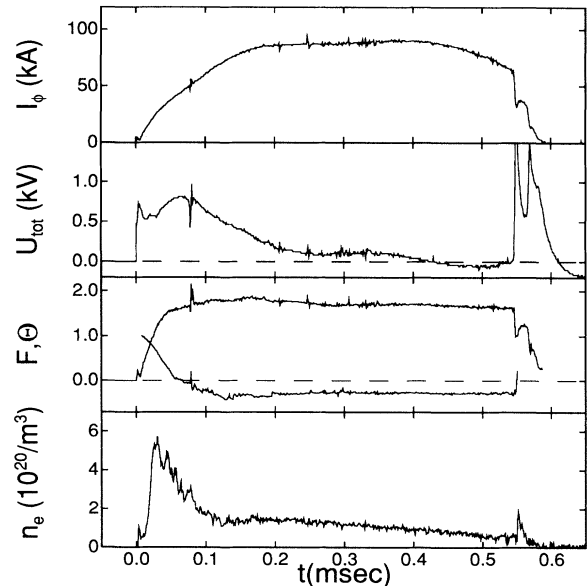


FIG. 1. Example of pulse data for discharge no. 25954 ($I_\phi \approx 90 \text{ kA}$, $\Theta \approx 1.7$). From top to bottom: Toroidal plasma current I_ϕ . Total loop voltage U_{tot} . Pinch parameter $\Theta = B_\theta(a)/\langle B_\phi \rangle$ (upper curve) and field reversal ratio $F = B_\phi(a)/\langle B_\phi \rangle$ (lower curve). Line average electron density n_e measured by interferometry.

with the particle confinement time, obtained from the hydrogen influx [9], and the energy confinement time for this current scan. In the analysis we have assumed a parabolic density profile and a flat temperature profile. Although these profiles may depend upon the operating conditions, the possible error of inferred trends in the calculated cross-sectionally averaged density and pressure, and thus in τ_p and τ_E , will be small, since we measure line averaged density and temperature. The ion temperature is assumed to be equal to the electron temperature. In Fig. 3 we show the scaling of the fraction of non-Spitzer input power $(P - P_S)/P$ and the magnetic fluctuation level $\delta B/B$ measured outside the vacuum vessel, with I/N . Fourier mode decomposition of the fluctuating edge magnetic field $\delta B/B$ reveals that the dominant mode numbers are $(m; n) = (1; -20, \dots, -15)$ and $(m; n) = (0; 1, \dots, 5)$. This activity has been identified as resistive tearing modes associated with the dynamo process.

In another series of experiments, Θ was varied from

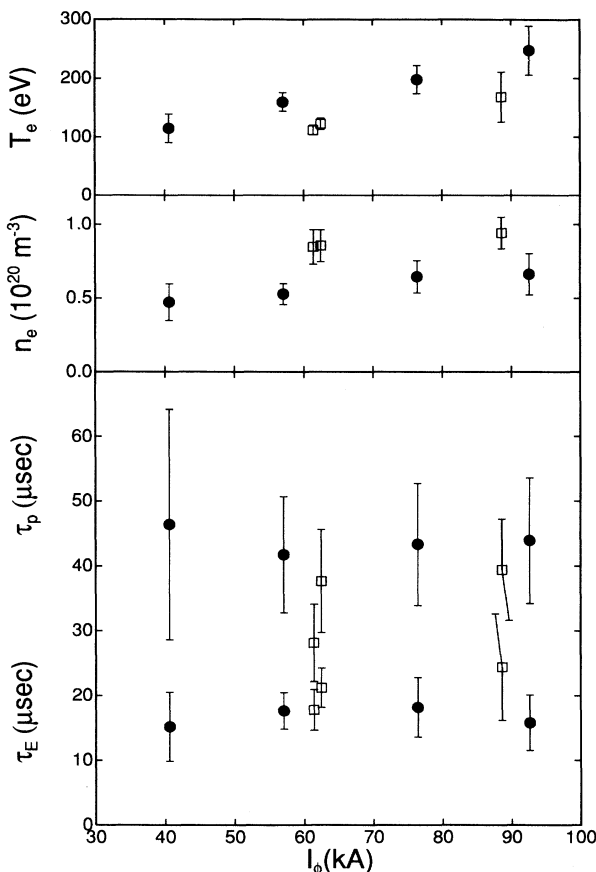


FIG. 2. From top to bottom: Line average electron temperature T_e . Line average electron density n_e . Particle confinement time τ_p (above the horizontal line) and energy confinement time τ_E (below the horizontal line) obtained at pinch parameter $\Theta \approx 1.7$. The different symbols indicate high $n_e \geq 0.75 \times 10^{20} \text{ m}^{-3}$ (\square) and low $n_e \leq 0.75 \times 10^{20} \text{ m}^{-3}$ (\bullet) discharges. The error bars represent three times the standard deviation of the ensemble averages of 20 consecutive discharges for each working point.

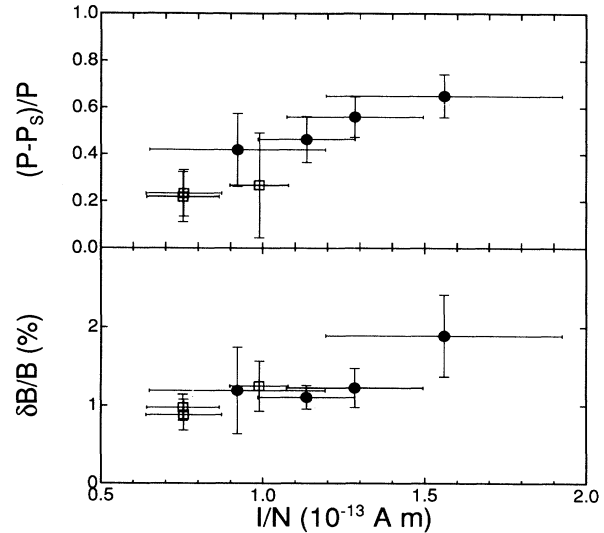


FIG. 3. Fraction of non-Spitzer input power $(P - P_S)/P$ and magnetic fluctuation level $\delta B/B$, obtained at pinch parameter $\Theta \approx 1.7$. The different symbols indicate high $n_e \geq 0.75 \times 10^{20} \text{ m}^{-3}$ (\square) and low $n_e \leq 0.75 \times 10^{20} \text{ m}^{-3}$ (\bullet) discharges. The error bars represent three times the standard deviation of the ensemble averages of 20 consecutive discharges for each working point.

1.6 to 2.6 for fixed $I/N = (0.7 \pm 0.1) \times 10^{-13} \text{ A m}$. In Fig. 4, we show $(P - P_S)/P$, $\delta B/B$, and particle and energy confinement times for this Θ scan.

In Figs. 2 and 4 we observe opposing trends for particle and energy confinement times. As a response to the increase of density at constant toroidal plasma current, τ_E is increased while τ_p is decreased. Within the Θ scan, τ_E is deteriorated at high Θ , whereas τ_p is improved. Although τ_E and τ_p are based upon assumed profiles, and τ_E is calculated with $T_i = T_e$, large variations in the temperature profile and in T_i/T_e would be required to convert the present trend of τ_E to one similar to τ_p . Any change in the density profile would affect both τ_E and τ_p alike. In the following, we propose an explanation for the observed opposing trends.

We note that the energy confinement time is slightly higher for high n_e data as compared to low n_e data for a given plasma current. Although the Spitzer input power is significantly reduced for the low n_e discharges, the non-Spitzer input power needed to sustain the configuration increases, resulting in higher total input power and, since the measured β remains essentially unchanged, slightly lower energy confinement time. Also within the Θ scan, the fraction of non-Spitzer input power increases. This enhanced dynamo activity is consistently observed in the increase of $\delta B/B$ with I/N for constant Θ and the increase of $\delta B/B$ with Θ for constant I/N . Hence we conclude that the scaling of τ_E is dominated by the input power associated with the sustainment of the magnetic configuration.

Concerning the scaling of particle confinement time with $\delta B/B$, it has been shown that tearing mode activity leads to stochasticization of the plasma. Particularly, at high Θ , overlapping of $m = 0$ and $m = 1$ magnetic

islands may cause stochastization of the entire plasma column [4, 10]. Accordingly, an increase in this activity would be expected to result not only in a degraded energy confinement time, but also in a deteriorated particle confinement time as Θ is increased. Instead, we observe that particle confinement is improved, although $\delta B/B$ increases with Θ . These observations suggest that dynamo related particle loss is only a minor part of the total particle loss in our experiment. Instead our observations indicate that the loss rate is dominated by transport associated with pressure-driven instabilities which establish the operational β . Here a possible candidate is pressure-driven resistive interchange modes which may be expected to arise in the vicinity of the reversal surface due to large pressure gradients in the edge region [11, 12]. In order to maintain resonance with the magnetic field in this region, such instabilities would possess very high toroidal mode numbers and thus result in high frequency field fluctuations. Accordingly, the magnetic signature of this activity would be more difficult to detect outside the vacuum vessel due to liner screening effects. Indeed, we observe that the scaling of the externally measured

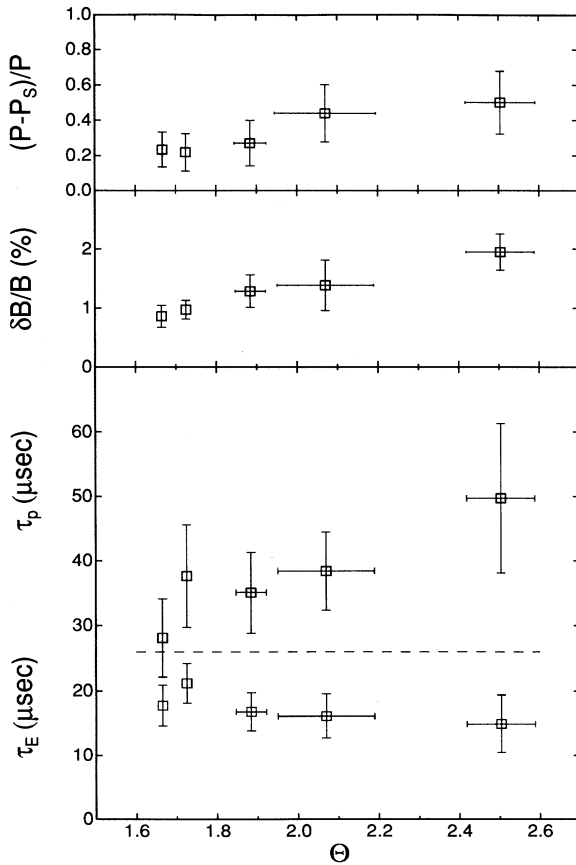


FIG. 4. From top to bottom: Fraction of non-Spitzer input power $(P - P_S)/P$. Magnetic fluctuation level, $\delta B/B$. Particle confinement time τ_p (above the horizontal line) and energy confinement time τ_E (below the horizontal line) obtained at $I/N \leq 0.8 \times 10^{-13}$ A m. The error bars represent three times the standard deviation of the ensemble averages of 20 consecutive discharges for each working point.

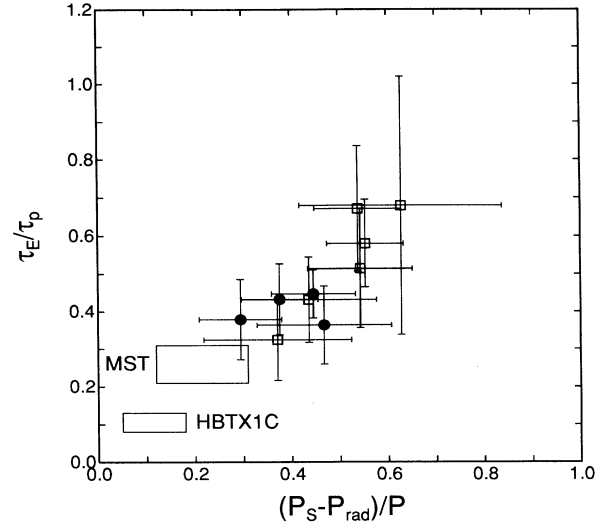


FIG. 5. Ratio of energy to particle confinement time as a function of the fraction of nonradiative Spitzer input power $(P_S - P_{\text{rad}})/P$ for current scan and Θ scan. The different symbols indicate high $n_e \geq 0.75 \times 10^{20} \text{ m}^{-3}$ (\square) and low $n_e \leq 0.75 \times 10^{20} \text{ m}^{-3}$ (\bullet) discharges. The data from MST and HBTX1C continue the trend within the Extrap-T1 data towards lower fraction of $(P_S - P_{\text{rad}})/P$. The error bars represent three times the standard deviation of the ensemble averages of 20 consecutive discharges for each working point.

fluctuation level $\delta B/B$ is dominated by the more global, and comparatively low n , tearing mode activity.

We can now explain the principal physics behind our observation that the particle confinement time is anticorrelated with the energy confinement time within the Θ scan, and when low n_e and high n_e series are compared. Spitzer heating power $\eta_S j^2$ acts to increase the pressure gradient, which in turn enhances localized pressure-driven instabilities. This enhanced pressure-driven activity results in an increased particle loss rate. Consequently a high fraction of direct heating leads to deteriorated particle confinement. If, in contrast, a large fraction of the input power is consumed by non-Spitzer processes, less power is available for direct heating and hence pressure-driven transport remains at a lower level. Although a fraction of this non-Spitzer input power may be dissipated in the plasma and contribute to heating [13], we find that this fraction cannot compensate for the reduction of direct heating when $(P - P_S)/P$ is increased. Since the scaling of τ_E is dominated by non-Spitzer input power, related to the dynamo activity, and the scaling of τ_p is coupled to direct heating and thus to pressure-driven instabilities, τ_E and τ_p are anticorrelated.

Although pressure-driven transport is essential for regulating β to the operational value, this transport may only be a minor part of the total power loss. In order to study this contribution, we present in Fig. 5 the ratio of energy to particle confinement time versus the fraction of nonradiative Spitzer input power $(P_S - P_{\text{rad}})/P$ for both the current scan and the Θ scan. Typically, 15–30% of the Spitzer input power in our experiment is measured to be radiated. In the limit of high $(P_S - P_{\text{rad}})/P$,

the energy and particle confinement times are comparable suggesting that the dominant power loss channel is thermal energy loss due to pressure-driven particle transport. In Fig. 5 we also include the range of values consistent with results obtained at the Madison Symmetric Torus ($R_0/a = 1.5 \text{ m}/0.52 \text{ m} = 2.9$) [14] and HBTX1C (Culham, Great Britain) ($R_0/a = 0.8 \text{ m}/0.26 \text{ m} = 3.1$) [15, 16] at low Θ , which appear to continue the trend in our data towards low τ_E/τ_p and low $(P_S - P_{\text{rad}})/P$. It should be emphasized, that the scaling of τ_E/τ_p is given by $(P_S - P_{\text{rad}})/P$ rather than the aspect ratio or the volume to surface ratio of the different devices.

From the general trend seen in Fig. 5 the following picture emerges. At a low fraction of $(P_S - P_{\text{rad}})/P$, the ratio τ_E/τ_p is also low. Here, the total energy losses cannot be explained by particles leaving the plasma carrying thermal energies. Hence, if convection is the dominant power loss channel in this regime, the energy carried by escaping particles has to be significantly larger than the representative thermal energy. This is consistent with the observation of high-energy electrons at the edge in

many RFP experiments (see [17] for a recent review). On the other hand, at a high fraction of direct heating, $(P_S - P_{\text{rad}})/P$, pressure-driven activity is enhanced, resulting in increased particle transport and a deteriorated particle confinement time. In this case, the resulting energy loss is a significant part of the total energy loss.

Our observations suggest that particle transport in the Extrap-T1 RFP is dominated by pressure-driven instabilities, which regulate the operational β value. The scaling of the energy confinement time, on the other hand, is dominated by the non-Spitzer input power required to sustain the magnetic configuration. Accordingly, τ_E and τ_p are found to be anticorrelated as the ratio of Spitzer to non-Spitzer input power is varied. At high fractions of Spitzer input power, convection of thermal particles can account for a major fraction of the total power loss.

This work has been supported by the European Communities under an association contract between EURATOM and the Swedish Natural Science Research Council.

-
- [1] H.A.B. Bodin, R.A. Krakowski, and S. Ortolani, *Fusion Technology* **10**, 307 (1986).
- [2] H.A.B. Bodin. *Nucl. Fusion* **30**, 1717 (1990).
- [3] E.J. Caramana, R.A. Nebel, and D.D. Schnack, *Phys. Fluids* **26**, 1305 (1983).
- [4] K. Kusano and T. Sato, *Nucl. Fusion* **30**, 2075 (1990).
- [5] Y.L. Ho and C.G. Craddock, *Phys. Fluids B* **3**, 721 (1991).
- [6] A.R. Jacobson and R.W. Moses, *Phys. Rev. A* **29**, 3335 (1984).
- [7] S. Mazur, P. Nordlund, K.-D. Zastrow, J.H. Brzozowski, and J.R. Drake (unpublished).
- [8] J.C. Sprott, *Phys. Fluids* **31**, 2266 (1988).
- [9] L.C. Johnson and E. Hinnov, *J. Quant. Spectrosc. Radiat. Transf.* **13**, 333 (1973).
- [10] D.D. Schnack, D.C. Barnes, Z. Mikic, D.S. Harned, E.J. Caramana, and R.A. Nebel, *Comput. Phys. Commun.* **43**, 17 (1986).
- [11] S.C. Prager, *Plasma Phys. Contr. Fusion* **32**, 903 (1990).
- [12] D.D. Schnack, H. Biglari, E.J. Caramana, B.A. Carreras, P.H. Diamond, F.Y. Gang, E. Hamieri, D.S. Harned, Y.L. Ho, J. McBride, R.A. Nebel, S.C. Prager, and H.R. Strauss, in *Plasma Physics and Controlled Nuclear Fusion Research, Nice, 1988*, Proceedings of the 12th International Conference (IAEA, Vienna, 1989).
- [13] N. Mattor, P.W. Terry, and S.C. Prager, *Comments Plasma Phys. Contr. Fusion* **15**, 65 (1992).
- [14] A. Almagri, S. Assadi, J. Beckstead, G. Chartras, M. Cudzinovic, D. Den Hartog, R. Dexter, S. Hokin, D. Holly, S. Prager, T. Rempel, J. Sarff, E. Scime, W. Shen, C. Spragins, C. Sprott, G. Starr, M. Stoneking, C. Watts, E. Klevans, R. Veerasingam, and R. Nebel, in *Physics of Alternative Confinement Schemes*, edited by S. Ortolani and E. Sindoni, International School of Plasma Physics "Piero Caldirola" (Società Italiana di Fisica, Varenna, 1990), p. 667.
- [15] P.G. Carolan, A. Patel, M.C. Sexton, and M.J. Walsh, *Nucl. Fusion* **30**, 2616 (1990).
- [16] B. Alper, C.A. Bunting, P.G. Carolan, A. Patel, and M.J. Walsh, in *Proceedings of the 17th EPS Conference on Controlled Fusion and Plasma Heating*, edited by G. Briffod, Adri Nijsen-Vis, and F.C. Schüller (The European Physical Society, Amsterdam, 1990).
- [17] S. Ortolani, *Plasma Phys. Contr. Fusion* **34**, 1903 (1992).